

DBHP: Trajectory Imputation in Multi-Agent Sports Using Derivative-Based Hybrid Prediction

Hanjun Choi^{1*}, Hyunsung Kim^{2, 3*}, Minho Lee⁴,
Chang-Jo Kim³, Jinsung Yoon³, and Sang-Ki Ko^{3, 5}

¹Korea Electronics Technology Institute, Seongnam, South Korea

²Korea Advanced Institute of Science and Technology, Daejeon, South Korea

³Fittogether Inc., Seoul, South Korea

⁴Saarland University, Saarbrücken, Germany

⁵University of Seoul, Seoul, South Korea

Abstract

Many spatiotemporal domains handle multi-agent trajectory data, but in real-world scenarios, collected trajectory data are often partially missing due to various reasons. While existing approaches demonstrate good performance in trajectory imputation, they face challenges in capturing the complex dynamics and interactions between agents due to a lack of physical constraints that govern realistic trajectories, leading to suboptimal results. To address this issue, the paper proposes a Derivative-Based Hybrid Prediction (DBHP) framework that can effectively impute multiple agents' missing trajectories. First, a neural network equipped with Set Transformers produces a naive prediction of missing trajectories while satisfying the permutation-equivariance in terms of the order of input agents. Then, the framework makes alternative predictions leveraging velocity and acceleration information and combines all the predictions with properly determined weights to provide final imputed trajectories. In this way, our proposed framework not only accurately predicts position, velocity, and acceleration values but also enforces the physical relationship between them, eventually improving both the accuracy and naturalness of the predicted trajectories. Accordingly, the experiment results about imputing player trajectories in team sports show that our framework significantly outperforms existing imputation baselines.

1 Introduction

Various spatiotemporal domains such as transportation, robotics, surveillance, and sports handle multi-agent trajectory data. In particular, with the recent advancement of computer vision and sensing technologies, a growing number of groups are collecting these types of data for various use cases. However, acquiring a complete set of trajectory data is still very challenging as there are many practical possibilities of missing partial trajectories. Wearable devices such as GPS trackers or motion sensors may experience temporary signal loss or malfunction, obstructing the collection of complete trajectory data. Similarly, computer vision systems often fail to detect agents in occluded regions or in low-lighting conditions. In particular, some domains pose unique challenges

for trajectory data collection, such as sports games with broadcasting camera view where players can disappear from the view depending on their relative positions to the ball.

The prevalence of missing values in multi-agent trajectory data calls for developing effective imputation techniques. One of the simple yet powerful solutions is to employ naive rule-based imputation methods such as forward/backward fill or linear interpolation. However, they cannot capture the complex dynamics and interactions between agents, resulting in suboptimal performance. On this account, many studies have proposed deep learning-based imputation methods that consider the spatiotemporal dependencies of the multi-agent movements. Though they aimed to improve accuracy by modeling such dependencies, most of them failed to significantly outperform the aforementioned naive baselines.

To address this issue, this paper proposes a framework named *Derivative-Based Hybrid Prediction* (DBHP) that imputes missing values in multi-agent trajectory data with high accuracy by enforcing the physical restrictions that realistic trajectories should satisfy. First, a deep neural network equipped with Set Transformers (Lee et al. 2019) and agent-wise bidirectional LSTMs (Hochreiter and Schmidhuber 1997) produces a series of predictions for missing values. In addition to this direct prediction of players' positions, the framework makes alternative predictions named *Derivative-Accumulating Predictions* (DAPs) by accumulating the predicted velocity and acceleration on the nearest observed positions for each missing segment in either direction. Then, the framework compromises by properly determining weights between the three types of predictions, i.e., neural network output, forward and backward DAPs, to make the best final prediction.

In the experiments, we evaluated the performance of our proposed framework on the three benchmark datasets collected from popular team sports: soccer, basketball, and American football. The experimental results demonstrate that our framework significantly outperforms existing baselines for multi-agent trajectory imputation in terms of accuracy. In particular, leveraging the derivative information was found to be effective in improving the physical plausibility of the imputed trajectories. Lastly, we present the additional possibility of utilizing our framework for other

*These authors contributed equally.

practical tasks, such as estimating match statistics with incomplete tracking data and forecasting future trajectories of players in sports.

In summary, the main contributions are as follows:

1. We introduce a multi-agent trajectory prediction model employing Set Transformers to ensure the permutation-equivariance of the agents. This architecture itself imputes missing values more accurately than previous state-of-the-art imputation models.
2. We propose the DAP mechanism that assembles smoother predictions than the outputs of the above neural network by leveraging the physical relationships between the position, velocity, and acceleration.
3. We propose the DBHP framework combining the above predictions by a weighted sum, where the weights are learned to maximize their relative advantages.
4. We demonstrate that the proposed framework has the capability to generalize across various sports games and is applicable to practical missing scenarios.

2 Related Work

Though many studies have proposed methods for imputing time series data, not all of them have addressed the specific challenges of multi-agent trajectories with complex interactions and dynamics. To name a few, TimesNet (Wu et al. 2023) and TIDER (Liu et al. 2023a) were designed to impute multivariate time series by modeling their temporal patterns such as multi-periodicity, seasonality, or local biases, but they are inappropriate for multi-agent spatiotemporal domains such as team sports since the behaviors of agents are highly uncertain without repeating patterns. SPIN (Marisca, Cini, and Alippi 2022) regarded the interaction between data acquired from multiple sensors, but it assumed that the sensors’ locations are fixed and thus is not applicable to our case of moving agents. Other studies have also addressed multi-agent trajectory imputation (Liu et al. 2023b; Choi and Lee 2023; Fang et al. 2024); however, they are limited to scenarios where agents’ positions remain fixed, making them unsuitable for our research involving moving agents.

On the other hand, recent studies designed to impute multi-agent trajectories focus on modeling agents’ complex interactions and dynamics. BRITS (Cao et al. 2018) proposed an RNN-based multi-agent imputation model that incorporates the observed features at missing time steps and past information, but it is prone to compounding errors caused by an incorrect prediction at an early stage. To address this issue, non-autoregressive imputation frameworks such as NAOMI (Liu et al. 2019) and NRTSI (Shan, Li, and Oliva 2023) were proposed, but they can only handle the case when all agents have the same missing period. Omidshafiei et al. (2022) recently proposed Graph Imputer that is applicable to practical scenarios such as missing player trajectories out of the camera view in team sports. Note that many studies (Yeh et al. 2019; Zhan et al. 2019; Kamra et al. 2020; Li et al. 2020; Sun et al. 2022b,a) have proposed frameworks for multi-agent trajectory prediction, but they are designed to forecast future trajectories in a

unidirectional manner and cannot leverage the information of the future observations.

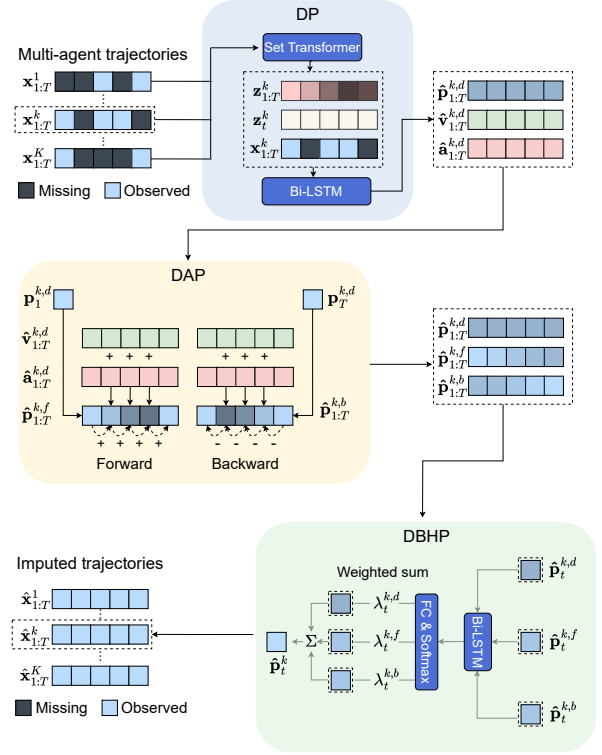


Figure 1: Overview of the proposed framework.

3 Proposed Framework

Our study about multi-agent trajectory imputation assumes a scenario where the missing time intervals of each agent could differ from those of others. To elaborate, let the trajectories of K players be $X_{1:T} = \{\mathbf{x}_{1:T}^k\}_{k=1}^K$, where each agent k 's input features \mathbf{x}_t^k at each time t consist of their (x, y) position $\mathbf{p}_t^k = (p_{t,x}^k, p_{t,y}^k)$, velocity $\mathbf{v}_t^k = (v_{t,x}^k, v_{t,y}^k)$, and acceleration $\mathbf{a}_t^k = (a_{t,x}^k, a_{t,y}^k)$. Here, the velocity and acceleration are calculated from the position values by the following approximations:

$$\mathbf{v}_t^k \approx \frac{\mathbf{p}_t^k - \mathbf{p}_{t-1}^k}{\Delta t}, \quad \mathbf{a}_t^k \approx \frac{\mathbf{v}_{t+1}^k - \mathbf{v}_t^k}{\Delta t} \quad (1)$$

where Δt is the difference between adjacent time steps.

In our scenario, each $\mathbf{x}_{1:T}^k$ has missing parts identified by a masking sequence $\mathbf{m}_{1:T}^k = (m_1^k, \dots, m_T^k)$ where $m_t^k = 1$ if \mathbf{x}_t^k is observed and 0 if it is missing. Note that the model may improperly exploit the information at the endpoints of masked segments in this setting since Eq. (1) uses the positional information at adjacent time steps when approximating the derivatives. To prevent this, we also mask the two frames adjacent to each missing segment to simulate a real situation where the model could not know the velocity and acceleration at those points.

Given this setting, an imputation model aims to take the incomplete data $\{\mathbf{m}_{1:T}^k \odot \mathbf{x}_{1:T}^k\}_{k=1}^K$ as input and produce imputed trajectories $\{\hat{\mathbf{x}}_{1:T}^k\}_{k=1}^K$. Combining these imputed trajectories with the observed fragments results in complete trajectories $\{\tilde{\mathbf{x}}_{1:T}^k\}_{k=1}^K$, i.e.,

$$\tilde{\mathbf{x}}_{1:T}^k = \mathbf{m}_{1:T}^k \odot \mathbf{x}_{1:T}^k + (\mathbb{1}_T - \mathbf{m}_{1:T}^k) \odot \hat{\mathbf{x}}_{1:T}^k, \quad (2)$$

for $k = 1, \dots, K$.

The novelty of the proposed framework lies in the mechanism of enhancing the model performance by integrating positions directly predicted by a neural network and those resulting from accumulating predicted derivatives (i.e., velocity and acceleration values). See Figure 1 illustrating the overall architecture of our framework.

Neural Network-Based Direct Prediction This section describes the neural network architecture producing naive predictions of imputed trajectories. It takes partially observed trajectories $\{\mathbf{m}_{1:T}^k \odot \mathbf{x}_{1:T}^k\}_{k=1}^K$ as an input and predicts each agent k 's full trajectory

$$\hat{\mathbf{x}}_{1:T}^{k,d} = \{(\hat{p}_{t,x}^{k,d}, \hat{p}_{t,y}^{k,d}, \hat{v}_{t,x}^{k,d}, \hat{v}_{t,y}^{k,d}, \hat{a}_{t,x}^{k,d}, \hat{a}_{t,y}^{k,d})\}_{t=1}^T, \quad (3)$$

where the superscript d stands for ‘‘direct prediction’’.

To build an effective neural architecture for modeling multiple trajectories, we should enforce a strong inductive bias called the *permutation-equivariance*. Since there is no semantic order of agents in our multi-agent systems, a permutation in the order of input agents should not affect the output value for each agent and only change the output order by the same permutation. We utilize the encoder module of the Set Transformer (Lee et al. 2019) to ensure the permutation-equivariance of outputs. A Set Transformer consists of an encoder that produces *permutation-equivariant* representations of multi-agent inputs and a decoder that produces a single *permutation-invariant* output shared for all agents. It is natural to only employ its encoder part for our permutation-equivariant task, but to improve the model performance, we also attach the permutation-invariant embedding that results from a full Set Transformer architecture, including the encoder and decoder parts.

To be specific, we obtain permutation-equivariant agent-wise embeddings $\{\mathbf{z}_t^k\}_{k=1}^K$ from the encoder of a Set Transformer and a single permutation-invariant embedding \mathbf{z}_t from a full Set Transformer for each time step t :

$$\begin{aligned} (\mathbf{z}_t^1, \dots, \mathbf{z}_t^K) &= \text{ST-Encoder}(m_t^1 \mathbf{x}_t^1, \dots, m_t^K \mathbf{x}_t^K), \\ \mathbf{z}_t &= \text{SetTransformer}(m_t^1 \mathbf{x}_t^1, \dots, m_t^K \mathbf{x}_t^K). \end{aligned} \quad (4)$$

Frame-by-frame application of the Set Transformer to the input features yields embeddings $\{(\mathbf{z}_t^1, \dots, \mathbf{z}_t^K, \mathbf{z}_t)\}_{t=1}^T$. Then, bidirectional LSTMs (Hochreiter and Schmidhuber 1997) sharing weights across agents extract the sequential information from the concatenated sequence $\{(\mathbf{x}_t^k, \mathbf{z}_t^k, \mathbf{z}_t)\}_{t=1}^T$ per agent k by updating joint hidden states:

$$\mathbf{h}_t^{k,f} = \text{LSTM}^f(\mathbf{x}_t^k, \mathbf{z}_t^k, \mathbf{z}_t; \mathbf{h}_{t-1}^{k,f}), \quad (5)$$

$$\mathbf{h}_t^{k,b} = \text{LSTM}^b(\mathbf{x}_t^k, \mathbf{z}_t^k, \mathbf{z}_t; \mathbf{h}_{t+1}^{k,b}). \quad (6)$$

Lastly, a fully-connected layer decodes the joint hidden state to output a prediction $\hat{\mathbf{x}}_t^{k,d}$ at each time t :

$$\hat{\mathbf{x}}_t^{k,d} = \text{FC}(\mathbf{h}_t^{k,f}, \mathbf{h}_t^{k,b}). \quad (7)$$

We call the prediction obtained in this phase the *direct prediction* (DP) and combine it with the other predictions from later phases to get more accurate final prediction.

Derivative-Accumulating Prediction We start from the following relationships between the position, velocity, and acceleration derived from Eq. (1):

$$\mathbf{p}_{t+1}^k \approx \mathbf{p}_t^k + \mathbf{v}_{t+1}^k \Delta t, \quad \mathbf{v}_{t+1}^k \approx \mathbf{v}_t^k + \mathbf{a}_t^k \Delta t, \quad (8)$$

Taking this into account, we compute *Derivative-Accumulating Prediction* (DAP) with improved stability by enforcing the physical relationships in Eq. (8), as an alternative to the direct imputation result. To elaborate, let (t_s, t_e) be an arbitrary missing segment for a player k . Then, we recursively predict positions inside the segment by accumulating velocities and accelerations in either direction. Along the forward direction, we start from the observed position $\mathbf{p}_{t_s}^k$ and recursively add predicted velocities and accelerations to obtain predictions $\hat{\mathbf{p}}_t^{k,f}$ based on Eq. (8):

$$\hat{\mathbf{p}}_{t_s}^{k,f} = \mathbf{p}_{t_s}^k \quad (9)$$

$$\hat{\mathbf{p}}_t^{k,f} \approx \hat{\mathbf{p}}_{t-1}^{k,f} + \hat{\mathbf{v}}_t^{k,d} \Delta t \quad (10)$$

$$\approx \hat{\mathbf{p}}_{t-1}^{k,f} + (\hat{\mathbf{v}}_{t-1}^{k,d} + \hat{\mathbf{a}}_{t-1}^{k,d} \Delta t) \Delta t, \quad t_s < t < t_e. \quad (11)$$

Likewise, we start from the observed position $\mathbf{p}_{t_e}^k$ at the opposite endpoint and recursively subtract the predicted derivatives to obtain *backward predictions* $\hat{\mathbf{p}}_t^{k,b}$.

Adopting DAPs instead of direct predictions carries several advantages. First, since the loss between these DAPs and the ground truth more penalizes unstable predictions of the velocity and acceleration, minimizing it improves the smoothness of the predicted derivatives. Considering that existing position-oriented imputation models suffer from fluctuating trajectories, these smooth derivatives have a clear advantage in that they result in more plausible positional predictions. Furthermore, enforcing the relationships between the physical quantities imposes an additional inductive bias to the model, which makes it more data-efficient.

Dynamic Hybrid Prediction Though DAP has a clear advantage over direct prediction, it also has a potential drawback called the *error compounding problem*. Namely, since we only rely on the observation at an endpoint as an anchor and the predicted derivatives that are accumulated on the anchor, the prediction error tends to grow as the number of iterations in Eq. (11) or its backward counterpart increases. On the contrary, the direct predictions resulting from Eq. (7) are robust against this problem since they do not strictly depend on predictions at other time steps.

To address this trade-off, we take a hybrid approach named *Derivative-Based Hybrid Prediction* (DBHP) to leverage the advantages of DP and DAP. That is, instead of solely relying on one of the aforementioned predictions $\{(\hat{\mathbf{p}}_{1:T}^{k,d}, \hat{\mathbf{p}}_{1:T}^{k,f}, \hat{\mathbf{p}}_{1:T}^{k,b})\}_{k=1}^K$, we compromise between them by

computing a weighted sum. More specifically, we first deploy an additional Bi-LSTM as well as the original Bi-LSTM per agent to obtain weights used to combine the DP and DAP. Specifically, we feed the predictions of three types $\hat{\mathbf{x}}_t^{k,d}$, $\hat{\mathbf{p}}_t^{k,f}$, $\hat{\mathbf{p}}_t^{k,b}$ together with the context embeddings \mathbf{z}_t^k , \mathbf{z}_t resulting from Eq. (4) per agent k and time step t into a Bi-LSTM to update hidden states:

$$\tilde{\mathbf{h}}_t^{k,f} = \text{LSTM}^f(\hat{\mathbf{x}}_t^{k,d}, \hat{\mathbf{p}}_t^{k,f}, \hat{\mathbf{p}}_t^{k,b}, \mathbf{z}_t^k, \mathbf{z}_t, \gamma_t; \tilde{\mathbf{h}}_{t-1}^{k,f}), \quad (12)$$

$$\tilde{\mathbf{h}}_t^{k,b} = \text{LSTM}^b(\hat{\mathbf{x}}_t^{k,d}, \hat{\mathbf{p}}_t^{k,f}, \hat{\mathbf{p}}_t^{k,b}, \mathbf{z}_t^k, \mathbf{z}_t, \gamma_t; \tilde{\mathbf{h}}_{t+1}^{k,b}). \quad (13)$$

where $\gamma_t = \exp(-\max\{0, \mathbf{W}_\gamma \delta_t + \mathbf{b}_\gamma\})$ is the temporal decay introduced in BRITS (Cao et al. 2018) to inform the model how far a given time step t is from the both observed endpoints. Since we want to fairly weigh the bidirectional DAPs, we use the time gap $\delta_t = (t - t_s, t_e - t)$ from both directions.

Lastly, a fully-connected layer with a softmax activation returns weights adding up to 1:

$$(\lambda_t^{k,d}, \lambda_t^{k,f}, \lambda_t^{k,b}) = \text{Softmax}(\text{FC}(\tilde{\mathbf{h}}_t^{k,f}, \tilde{\mathbf{h}}_t^{k,b})). \quad (14)$$

Based on these weights, the model yields a final prediction:

$$\hat{\mathbf{p}}_t^k = \lambda_t^{k,d} \hat{\mathbf{p}}_t^{k,d} + \lambda_t^{k,f} \hat{\mathbf{p}}_t^{k,f} + \lambda_t^{k,b} \hat{\mathbf{p}}_t^{k,b}, \quad (15)$$

and combine the resulting trajectories with the observed fragments by Eq. (2) as follows:

$$\hat{\mathbf{x}}_{1:T}^k = \mathbf{m}_{1:T}^k \odot \mathbf{x}_{1:T}^k + (\mathbb{1}_T - \mathbf{m}_{1:T}^k) \odot \hat{\mathbf{x}}_{1:T}^k, \quad (16)$$

where $\hat{\mathbf{x}}_t^k = (\hat{p}_{t,x}^k, \hat{p}_{t,y}^k, \hat{v}_{t,x}^{k,d}, \hat{v}_{t,y}^{k,d}, \hat{a}_{t,x}^{k,d}, \hat{a}_{t,y}^{k,d})$.

Loss function In our framework, the more accurate the prediction at each stage, the more reliable the final DBHP outputs. Hence, we minimize not only the loss between the final prediction and the true trajectories, but also terms to compare the auxiliary predictions with the ground truth. That is, we compute the mean absolute error (MAE) for the DP, DAP, and the final hybrid prediction. We name the MAE loss function for DP, forward and backward DAPs and the final hybrid prediction as \mathcal{L}^d , \mathcal{L}^f , \mathcal{L}^b , and \mathcal{L}^h , respectively. Finally, the proposed DBHP model is trained by minimizing

$$\mathcal{L}^{\text{DBHP}} = \mathcal{L}^d + \mathcal{L}^f + \mathcal{L}^b + \mathcal{L}^h. \quad (17)$$

4 Main Experiments

One of the most challenging domains for multi-agent trajectory prediction is team sports since the movements and interactions of players are highly dynamic and complex, and the example is illustrated in Figure 2. Thus, we conduct experiments on team sports data to evaluate the imputation performance of our proposed framework on this challenging domain.

4.1 Experimental Settings

Data preparation In the experiments, we independently train models and evaluate the performance on three public datasets collected from three popular team sports: soccer, basketball, and American football. The soccer dataset is provided by Metrica Sports¹ and contains tracking data of 22

¹<https://github.com/metrica-sports/sample-data>

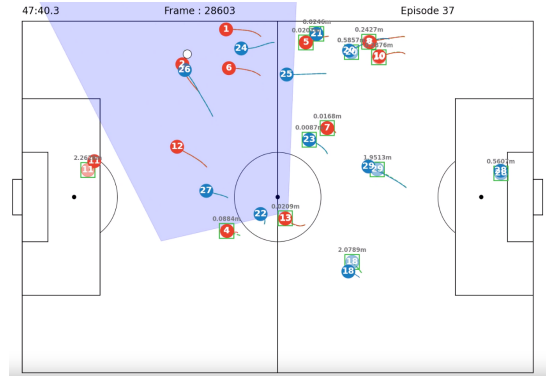


Figure 2: Example of a simulated camera view and imputed trajectories in soccer. The shaded area indicates the observed region on the pitch. The model imputes the trajectories of players outside this region, where translucent circles represent the predicted locations.

players collected from 3 matches. For basketball, we use 100 matches among 631 matches of SportsVU’s NBA dataset², where each match contains trajectories of 10 players. The American football dataset is from the Kaggle competition³ with NFL’s Next Gen Stats data, where we adopt the preprocessed version⁴ of NRTSI (Shan, Li, and Oliva 2023) containing 9,543 5-second time series. The original sampling rates of the three datasets are 25Hz, 25Hz, and 10Hz, respectively, but we downsampled them to a common rate of 10Hz for consistency. For soccer and basketball, 200 frames were used as input data with 22 players and 10 players, respectively, while for American football, 50 frames and 6 offensive players were used as input data.

Missing scenarios To evaluate the model performance on various missing patterns, we consider the following three scenarios that may occur during data acquisition processes:

- Uniform missing scenario: All players have missing values at the same time interval. Note that among the baselines, NAOMI (Liu et al. 2019) and NRTSI (Shan, Li, and Oliva 2023) are designed to only handle this scenario and not capable of the following other scenarios.
- Agent-wise missing scenario: Individual players have missing values at different time intervals.
- Broadcasting camera scenario: A virtual camera follows the ball and only captures the players inside the camera view, resulting in missing values for the remaining players. Following Graph Imputer (Omidshafiei et al. 2022), we conduct an experiment only on the soccer dataset for this scenario.

Figure 3 illustrates examples of masking matrices of the soccer dataset used in each missing scenario. Since our task is to impute trajectories given the observed data before

²<https://github.com/linouk23/NBA-Player-Movements>

³<https://www.kaggle.com/competitions/nfl-big-data-bowl-2021>

⁴https://github.com/lupalab/NRTSI/tree/main/codes_stochastic

Dataset	Soccer						Basketball				American Football			
Scenario	Uniform		Agent-wise		Camera		Uniform		Agent-wise		Uniform		Agent-wise	
Metric	PE	SCE	PE	SCE	PE	SCE	PE	SCE	PE	SCE	PE	SCE	PE	SCE
L. Interp.	3.8406	0.1299	5.0752	0.1631	3.1083	0.0993	3.3481	0.1483	4.4992	0.1787	0.8897	1.1063	1.5128	1.0641
C. Spline.	2.2085	0.0867	11.4647	0.2939	1.9209	0.0547	2.3114	0.1025	10.3857	0.2715	0.7448	0.9463	1.2041	0.5306
BRITS	7.4859	3.9089	5.7266	2.9627	7.4208	4.1967	2.9085	1.0521	2.4238	0.5397	1.7990	10.9459	1.7527	10.6807
NAOMI	4.5343	3.9793	N/A	N/A	N/A	N/A	1.5254	0.3230	N/A	N/A	0.9692	2.3112	N/A	N/A
NAOMI-ST	2.0147	1.3561	N/A	N/A	N/A	N/A	1.5038	0.0818	N/A	N/A	0.5889	0.6367	N/A	N/A
NRTSI	3.1791	0.0854	N/A	N/A	N/A	N/A	2.5291	0.0734	N/A	N/A	0.5158	0.2989	N/A	N/A
CSDI	3.4295	0.1586	4.0279	0.1305	3.5181	0.2132	2.2558	0.0631	2.3471	0.0563	0.5558	0.4905	0.6182	0.4288
G. Imputer	4.6511	0.1191	5.6011	0.1508	3.6512	0.0934	2.8305	0.1066	2.5859	0.0700	0.8899	1.1023	1.5128	1.0631
DBHP-TF	1.4384	0.0555	2.0286	0.0551	1.2849	0.0377	1.1585	0.0495	1.4701	0.0411	0.1752	0.1229	0.2389	0.1077
DBHP	1.3205	0.0516	1.9832	0.0535	1.2296	0.0374	0.9727	0.0438	1.3862	0.0381	0.1542	0.1126	0.2104	0.0967

Table 1: Performance of trajectory imputation models on different datasets and missing scenarios.



Figure 3: Visualization of example masking matrices for three different missing scenarios.

and after the missing intervals, we make the first and last five frames of each window not missed as in the previous works (Liu et al. 2019; Omidshafiei et al. 2022; Shan, Li, and Oliva 2023). It is also worth mentioning that we used a dynamic missing rate ranging from 0.1 to 0.9 during training, and evaluated it with a fixed missing rate of 0.5 during testing to enable the model to learn across various missing rate scenarios.

Models and evaluation metrics In the experiments, we compare the imputation performance with several baseline models. Additionally, we also conduct experiments on DBHP-TF, which utilizes a Transformer in the encoder part of DBHP. Note that for models such as BRITS, CSDI and NAOMI that do not preserve permutation-equivariance of the order of input players, we sort trajectories by the sum of average x and y coordinates to ensure permutation robustness. Therefore, to verify the importance of permutation-equivariance in the multi-agent trajectory imputation task, We conduct additional experiments on the NAOMI-ST model, which adds a set transformer embedding to the NAOMI.

To evaluate the performance of our framework and the baselines, we adopt the following two metrics:

- Position error (PE): the average Euclidean distance between the true and predicted positions.
- Step change error (SCE) (Liu et al. 2019; Shan, Li, and

Oliva 2023): the average absolute difference between the variance of the true and predicted velocities to assess the naturalness of imputed trajectories.

4.2 Experimental Results

Table 1 exhibits the trajectory imputation performance of the aforementioned models on different datasets and missing scenarios. Experimental results show that our proposed framework significantly outperforms other baselines. Since the lack of permutation equivalence is considered as one of the main limitations of baselines, we attach the Set Transformer encoder to NAOMI which is a competitive baseline model and report the result with the name NAOMI-ST. The comparison between NAOMI and NAOMI-ST shows that the permutation equivariance is indeed an important cause. We also replace Bi-LSTM from DBHP which is employed for sequential modeling by a transformer module and report the result with the name DBHP-TF. The comparison between DBHP-TF and DBHP validates our choice of Bi-LSTM for sequential modeling as DBHP performs slightly better than DBHP-TF. Figure 4 visualizes the imputed trajectories resulting from major baselines with our model.

Another observed advantage of our proposed framework is data efficiency. For the soccer dataset with only two matches of training data, other neural network baselines are even worse than the linear interpolation. Given that baselines such as NAOMI and NRTSI outperform the linear interpolation on both basketball and American football datasets with sufficient training data, the main reason for their poor performance on the soccer dataset appears to be the shortage of training data. On the other hand, our framework exhibits way better performance than all baselines including the linear interpolation on the soccer dataset as well as the basketball and American football datasets. Considering the difficulty in acquiring complete trajectory data in many domains, we believe that our framework can be efficiently applied to various domains even with a small amount of training data.

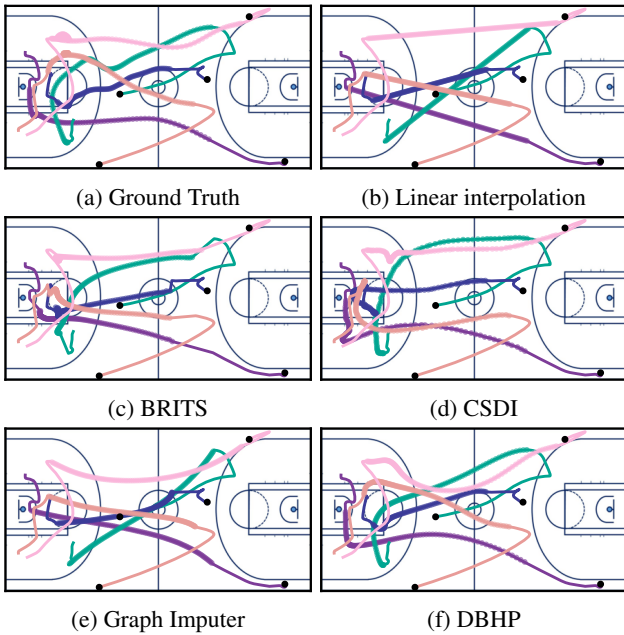


Figure 4: Comparison of ground truth and imputed trajectories for the basketball dataset.

4.3 Ablation Studies

In addition to the main experiments, we have carried out ablation studies to explore the impacts of each component introduced in DBHP framework. We also conduct comparative analyses on different window sizes and missing rates for our proposed model. For simplicity, both experiments were conducted only on the soccer dataset.

Impact of the derivative information as input To empirically justify the use of derivative features in DP and DAP, we compared the performance of our dynamic DBHP on the broadcasting camera scenario with those trained without accelerations (i.e., using positions and velocities) and even velocities (i.e., only using positions) of observed trajectories. Furthermore, we made DP only predict positions and velocities, and DAP estimate positions only based on predicted velocities. We trained the models with these “velocity-only” DAP and compared the performance with their counterparts that exploited predicted acceleration values.

DP Feats.	DAP Feats.	$\hat{p}_t^{k,d}$	$\hat{p}_t^{k,f}$	$\hat{p}_t^{k,b}$	\hat{p}_t^k
pos.	vel.	4.0008	2.8203	2.8261	2.5549
pos.	vel. & acc.	2.9119	2.6973	2.6858	2.4954
pos. & vel.	vel.	1.6600	1.5742	1.5590	1.4025
pos. & vel.	vel. & acc.	1.6235	1.5731	1.5670	1.4013
all feats.	vel.	1.6713	1.4985	1.5595	1.2644
all feats.	vel. & acc.	1.4963	1.4122	1.3982	1.2296

Table 2: Position errors of the components of the dynamic DBHP in Eq. 15 trained using different subsets of features.

According to Table 2, using velocities and accelerations as input features of DP clearly helps the model better predict missing trajectories. In particular, models that only observe positional information suffer from significant performance degradation. We think this comes from the architecture of DP that first independently encodes multi-agent contexts for each time step by Set Transformers and then connects sequential information by agent-wise Bi-LSTMs. Here, taking derivatives as input makes the Set Transformers consider some information of adjoining time steps, resulting in more comprehensive context embeddings than those only observing positions.

Results on different window sizes and missing rates We compare the model performance on scenarios with different window sizes and missing rates. A longer window allows the model to observe more data points but leads to an increase in the maximum length of a missing segment. Meanwhile, a higher missing rate increases the overall ratio of the missing frames to the observed frames. To be specific, we independently changed the size of the sliding windows from 50 to 600 and the missing rate from 0.3 to 0.7 of the agent-wise missing scenario. Then, we measured the position errors of models for each combination. We also evaluated the performance of the broadcasting camera scenario for each window size and reported the missing rate of it.

WS \ MR	0.3	0.5	0.7	Camera (MR)
50	0.0691	0.1158	0.1552	0.0841 (0.4569)
100	0.3561	0.5948	0.8047	0.4622 (0.5138)
200	1.2805	2.0491	2.5556	1.1711 (0.5375)
300	2.3129	3.2746	4.0821	1.5993 (0.5454)
600	4.2597	5.9329	7.2485	2.1410 (0.5540)

Table 3: Position errors of the DBHP trained for and applied to scenarios with different window sizes and missing rates. The number inside each parenthesis in the rightmost column indicates the missing rate of the corresponding broadcasting camera scenario.

Agreeing with our intuition, Table 3 shows that the model becomes less accurate as either the window size or the missing rate increases. In particular, the position error of the agent-wise missing scenario becomes much larger for a longer window, even with a small missing rate. This is because some players may miss most frames in the process of randomly distributing the total number of missing frames to individuals. Accordingly, in a longer window, the model has to predict the players’ stochastic movements for tens of seconds, resulting in a large error due to its inherent difficulty. Meanwhile, in the broadcasting camera scenario, the maximum length of a missing segment does not significantly change according to the window size. This results in robust performance against varying window sizes, implying that our framework can be reliably applied to real-world broadcasting data.

5 Applications

In this section, we explore the possibility of leveraging our framework for practical tasks. As examples, we present two promising applications in soccer domain: pitch control analysis (Spearman et al. 2017) and approximating match statistics from incomplete tracking data.

Pitch control analysis We show that our framework can be used to perform pitch control (Spearman et al. 2017) analysis, which is a well-established technique in soccer analytics, in partially-observable settings. Pitch control can be used to quantify how soccer players control regions on the pitch at each time step by relying on physics-based modeling. In Figure 5, the pitch image corresponding to each model represents the difference between pitch control results where one from the ground-truth trajectory and the other from the partial observations where the missing trajectory is imputed by the model. If a specific area of the pitch is shaded with a darker color, it indicates a greater difference. Figure 5 shows that DBHP achieves the most similar result compared to other baselines.

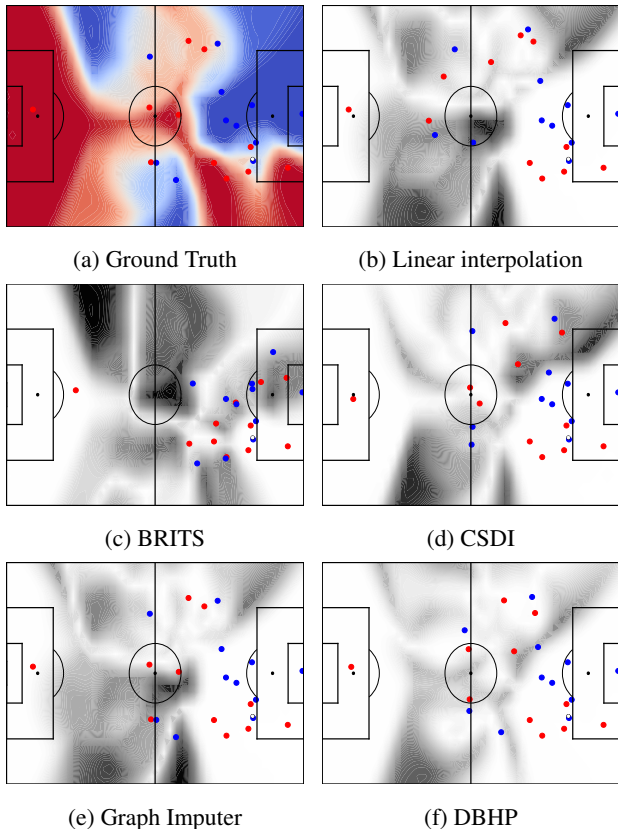


Figure 5: Absolute error of pitch control analysis.

Approximation of match statistics In this section, we explore how accurately our method can estimate statistics for the entire match when imputed trajectories are merged with known observations. To elaborate, we compare the *total distance* covered by a player and the *number of sprints* esti-

mated by each method, as they are widely used as indicators for players’ physical performance or fitness. We first compute velocities from the observed/imputed positions based on Eq. 1 and obtain speed values by calculating the norms of these velocity vectors. Then, we compute the distance covered by each player by summing up the speed values multiplied by $\Delta t = 0.1s$. For the latter, if a player runs faster than 6 m s^{-1} for consecutive frames, we detect his/her movement during the frames as a *sprint*. Then, we count the number of sprints the player made during the given period.

		Distance (m)		# Sprints	
Model	OR	Mean	MAPE	Mean	MAPE
True	-	11,093.5	-	41.49	-
L. Interp.	1.55%	10,049.2	9.28%	38.13	7.97%
BRITS	34.68%	10,559.7	4.57%	52.07	30.95%
G. Imputer	5.23%	8,972.1	19.15%	37.85	9.80%
DBHP	0.01%	10,931.4	1.48%	40.41	4.25%

Table 4: Player statistics estimated by different models and their mean absolute percentage errors (MAPE) for the soccer test data. OR stands for the outlier rate, i.e., the proportion of outlier frames with large speed or acceleration values.

For evaluation, we use the soccer test data consisting of the half of a match and assume the broadcasting camera scenario. Since players played for different time periods, we normalize each player’s statistics by 90 minutes and calculate the averages of such normalized values estimated by DBHP and other baselines, respectively.

According to Table 4, DBHP provides accurate estimates close to the ground truth with few outliers. Especially considering that other methods either suffer from a huge number of outliers (BRITS) or inaccurate distance measures (linear interpolation and Graph Imputer), it is obvious that our model takes clear advantage of smooth prediction of velocities. In a nutshell, our framework is practical in that it can provide reliable statistics (with incomplete tracking data) which originally require entire player trajectories.

6 Conclusions

This paper proposes DBHP, a trajectory imputation framework that imputes missing values of multiple agents with improved quality. It consists of a neural network that makes an initial prediction in a permutation-equivariant manner and an additional scheme for incorporating derivatives to refine the imputation results. The experiments conducted on the sports datasets with various missing scenarios demonstrate the effectiveness of our approach in imputing multi-agent trajectories with not only higher accuracy but also improved reality. Though our study focused on the performance of our framework on team sports data, we believe it can also be applied to other spatiotemporal domains. Future work will further investigate its application to practical tasks in team sports and other domains that require complete trajectories of multiple agents.

References

- Cao, W.; Wang, D.; Li, J.; Zhou, H.; Li, L.; and Li, Y. 2018. BRITS: Bidirectional recurrent imputation for time series. In *Advances in Neural Information Processing Systems* 31.
- Choi, M.; and Lee, C. 2023. Conditional Information Bottleneck Approach for Time Series Imputation. In *The Twelfth International Conference on Learning Representations*.
- Fang, S.; Wen, Q.; Luo, Y.; Zhe, S.; and Sun, L. 2024. BayOTIDE: Bayesian Online Multivariate Time series Imputation with functional decomposition.
- Hochreiter, S.; and Schmidhuber, J. 1997. Long short-term memory. *Neural Computation*.
- Kamra, N.; Zhu, H.; Trivedi, D.; Zhang, M.; and Liu, Y. 2020. Multi-agent trajectory prediction with fuzzy query attention. In *Advances in Neural Information Processing Systems* 33.
- Kingma, D. P.; and Welling, M. 2014. Auto-encoding variational bayes. In *Proceedings of the 2nd International Conference on Learning Representations*.
- Kipf, T. N.; Fetaya, E.; Wang, K.; Welling, M.; and Zemel, R. S. 2018. Neural relational inference for interacting systems. In *Proceedings of the 35th International Conference on Machine Learning*.
- Le, H. M.; Carr, P.; Yue, Y.; and Lucey, P. 2017. Data-driven ghosting using deep imitation learning.
- Lee, J.; Lee, Y.; Kim, J.; Kosiorek, A. R.; Choi, S.; and Teh, Y. W. 2019. Set Transformer: A Framework for attention-based permutation-invariant neural networks. In *Proceedings of the 36th International Conference on Machine Learning*.
- Li, J.; Yang, F.; Tomizuka, M.; and Choi, C. 2020. Evolve-Graph: Multi-agent trajectory prediction with dynamic relational reasoning. In *Advances in Neural Information Processing Systems* 33.
- Liu, S.; Li, X.; Cong, G.; Chen, Y.; and Jiang, Y. 2023a. Multivariate time-series imputation with disentangled temporal representations. In *The 11th International Conference on Learning Representations*.
- Liu, S.; Li, X.; Cong, G.; Chen, Y.; and Jiang, Y. 2023b. Multivariate time-series imputation with disentangled temporal representations. In *The Eleventh international conference on learning representations*.
- Liu, Y.; Yu, R.; Zheng, S.; Zhan, E.; and Yue, Y. 2019. NAOMI: Non-autoregressive multiresolution sequence imputation. In *Advances in Neural Information Processing Systems* 32.
- Marisca, I.; Cini, A.; and Alippi, C. 2022. Learning to reconstruct missing data from spatiotemporal graphs with sparse observations. In *Advances in Neural Information Processing Systems* 35.
- Omidshafiei, S.; Hennes, D.; Garnelo, M.; Wang, Z.; Recasens, A.; Tarassov, E.; Yang, Y.; Elie, R.; Connor, J.; Muller, P.; Mackraz, N.; Cao, K.; Moreno, P.; Sprechmann, P.; Hassabis, D.; Graham, I.; Spearman, W.; Heess, N.; and Tuyls, K. 2022. Multiagent off-screen behavior prediction in football. *Scientific Reports*.
- Shan, S.; Li, Y.; and Oliva, J. B. 2023. NRTSI: Non-recurrent time series imputation. In *IEEE International Conference on Acoustics, Speech and Signal Processing*.
- Spearman, W.; Basye, A.; Dick, G.; Hotovy, R.; and Pop, P. 2017. Physics-based modeling of pass probabilities in soccer. In *MIT Sloan Sports Analytics Conference*.
- Sun, F.; Kauvar, I.; Zhang, R.; Li, J.; Kochenderfer, M. J.; Wu, J.; and Haber, N. 2022a. Interaction modeling with multiplex attention. In *Advances in Neural Information Processing Systems* 35.
- Sun, Q.; Huang, X.; Gu, J.; Williams, B. C.; and Zhao, H. 2022b. M2I: From factored marginal trajectory prediction to interactive prediction. In *IEEE/CVF Conference on Computer Vision and Pattern Recognition*.
- Teranishi, M.; Tsutsui, K.; Takeda, K.; and Fujii, K. 2022. Evaluation of creating scoring opportunities for teammates in soccer via trajectory prediction. In *ECML PKDD Workshop on Machine Learning and Data Mining for Sports Analytics*.
- Wu, H.; Hu, T.; Liu, Y.; Zhou, H.; Wang, J.; and Long, M. 2023. TimesNet: Temporal 2d-variation modeling for general time series analysis. In *The 11th International Conference on Learning Representations*.
- Wu, Y.; and Swartz, T. 2023. Evaluation of off-the-ball actions in soccer. *Statistica Applicata - Italian Journal of Applied Statistics*.
- Yeh, R. A.; Schwing, A. G.; Huang, J.; and Murphy, K. 2019. Diverse generation for multi-agent sports games. In *IEEE/CVF Conference on Computer Vision and Pattern Recognition*.
- Zhan, E.; Zheng, S.; Yue, Y.; Sha, L.; and Lucey, P. 2019. Generating multi-agent trajectories using programmatic weak supervision. In *Proceedings of the 7th International Conference on Learning Representations*.

A Appendix / Supplemental Material

A.1 Dataset Statistics

Dataset	Split	# Matches	# Episodes	# Frames
Soccer	Train.	2	134	70,119
	Valid.	0.5	28	20,690
	Test	0.5	34	21,424
Basketball	Train.	70	4,835	1,843,329
	Valid.	10	687	249,474
	Test	20	1,362	529,764
A. Football	Train.	-	8,500	425,000
	Valid.	-	1,043	52,150
	Test	-	-	-

Table 5: Datasets used in our experiments.

Table 5 provides details on each dataset, including the number of matches, episodes, and frames. The term *episode* is defined as a time interval during which the game was in play without any pauses or missing frames. For the soccer dataset, matches are divided into episodes based on the times at which the game was paused and resumed. In contrast, for the basketball dataset, since most out-of-play situations have already been excluded, an episode is defined as the time interval that contains all consecutive time points. When training models with either the soccer or basketball datasets, we select episodes that are at least 200 frames in length and create a PyTorch Dataset by sliding a 200-frame window (equivalent to 20 seconds) across each episode with a 5-frame (0.5 seconds) overlap, resulting in adjoining windows that share 195 frames. For the American football dataset, we follow the NRTSI setting, treating each preprocessed 5-second window as an episode.

A.2 Hybrid with static or Dynamic Weights

Dataset	Soccer						Basketball				American Football			
	Uniform		Agent-wise		Camera		Uniform		Agent-wise		Uniform		Agent-wise	
Metric	PE	SCE	PE	SCE	PE	SCE	PE	SCE	PE	SCE	PE	SCE	PE	SCE
DBHP-S	1.3564	0.0514	2.0192	0.0569	1.3187	0.0589	0.9744	0.0434	1.3882	0.0378	0.1681	0.1378	0.2184	0.1037
DBHP-S2	1.3261	0.0521	1.9891	0.0537	1.2376	0.0379	0.9739	0.0442	1.3885	0.0388	0.1571	0.1159	0.2127	0.0978
DBHP	1.3205	0.0516	1.9832	0.0535	1.2296	0.0374	0.9727	0.0438	1.3862	0.0381	0.1542	0.1126	0.2104	0.0967

Table 6: Performance of hybrid prediction models on different datasets and missing scenarios.

In this section, we conduct additional experiments to validate the necessity of dynamic hybrid prediction in the multi-agent trajectory imputation task. Accordingly, we introduce another two different hybrid schemes, DBHP-S and DBHP-S2, which use predefined static weights instead of learnable weights.

As defined in the Derivative-Accumulating Prediction in Section 3, let (t_s, t_e) be an arbitrary missing segment for player k . The DBHP-S and DBHP-S2 are based on the assumption that DAPs become less accurate as they correspond to time steps further away from the observed anchors (i.e., $p_{t_s}^k$ or $p_{t_e}^k$). For DBHP-S, we assign large weights to forward DAPs near the left endpoint, to DP in the middle, and to backward DAPs near the right endpoint, respectively. Then, we combine the DP and bidirectional DAPs in either direction by predetermined weights as follows:

$$\hat{\mathbf{p}}_t^{k,s} = \begin{cases} \frac{t-t_s}{t_m-t_s} \hat{\mathbf{p}}_t^{k,d} + \frac{t_m-t}{t_m-t_s} \hat{\mathbf{p}}_t^{k,f} & \text{if } t_s < t < t_m, \\ \frac{t_e-t}{t_e-t_m} \hat{\mathbf{p}}_t^{k,d} + \frac{t-t_m}{t_e-t_m} \hat{\mathbf{p}}_t^{k,b} & \text{if } t_m \leq t < t_e. \end{cases} \quad (18)$$

where $t_m = (t_s + t_e)/2$ is the midpoint of the segment. For DBHP-S2, we assign large weights to forward DAP near the left endpoint and to backward DAP near the right endpoint. For a player k 's missing segment (t_s, t_e) , we combine DAPs in either direction using predetermined weights as follows:

$$\hat{\mathbf{p}}_t^{k,s2} = \frac{t_e-t}{t_e-t_s} \hat{\mathbf{p}}_t^{k,f} + \frac{t-t_s}{t_e-t_s} \hat{\mathbf{p}}_t^{k,b}. \quad (19)$$

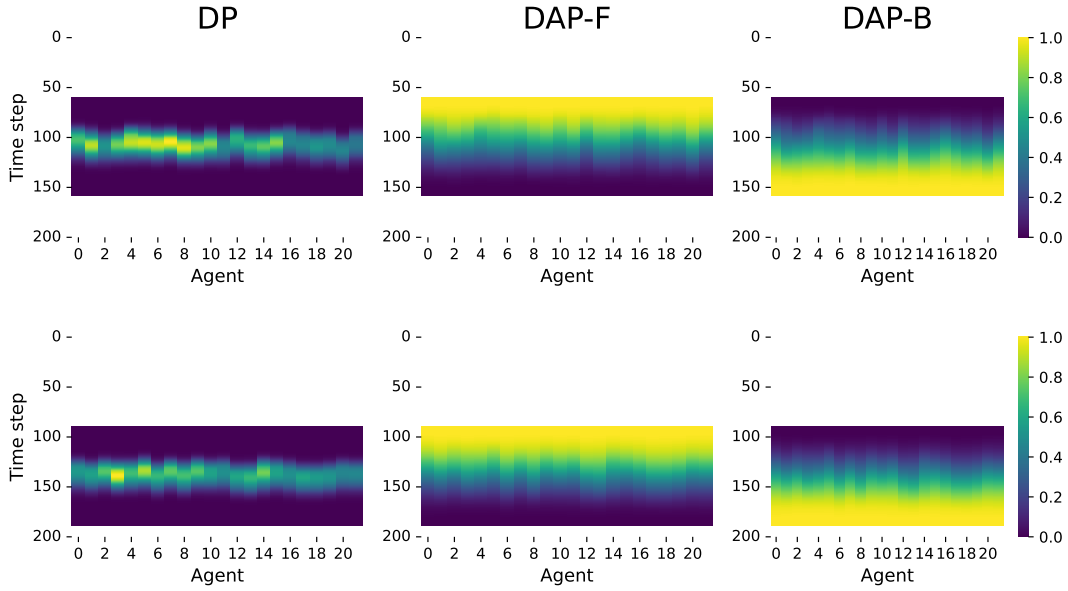


Figure 6: Visualization of the weights assigned to each DP, DAP-F, and DAP-B for the DBHP model.

Table 6 shows the trajectory imputation performance of different hybrid prediction models. In most cases, the performance of our proposed DBHP, achieves better results than that of other hybrid models. Figure 6 illustrates the visualization of the weights assigned to each prediction in the DBHP model. The weights of DAPs are heavily assigned to the near the endpoints of the missing segment, while the weights of DP are significantly assigned to the middle.

These results demonstrate that our DBHP model can appropriately combine each prediction to fit diverse situations such as the agents' intense movements or the length of missing segments. To be specific, in situations where an agent abruptly changes direction or undergoes sudden changes in speed and acceleration, the DAP's predictions may become inaccurate. In these cases, utilizing the DP prediction could be more accurate. Additionally, as the length of the missing segment increases, the risk of error compounding in the DAP's predictions also rises. For these reasons, it is essential to design a model that can appropriately adapt to these situations when given partial trajectories in multi-agent trajectory imputation task.

A.3 Impact of loss functions

Loss	DP	DAP-F	DAP-B	DBHP-S	DBHP-S2	DBHP
\mathcal{L}^d	1.4903	7.6358	7.6371	2.1680	3.0482	3.9707
\mathcal{L}^f	64.3613	1.4092	1.8953	32.4138	1.4077	17.1049
\mathcal{L}^b	62.0796	1.8719	1.4615	31.9822	1.4544	17.5418
$\mathcal{L}^d + \mathcal{L}^f$	1.3382	1.3511	1.9678	1.3273	1.3897	1.4616
$\mathcal{L}^d + \mathcal{L}^b$	1.3799	2.0537	1.3944	1.3824	1.4681	1.5356
\mathcal{L}^h	59.3137	3.6357	3.6915	30.1380	1.5318	1.3311
$\mathcal{L}^d + \mathcal{L}^f + \mathcal{L}^b + \mathcal{L}^h$	1.4963	1.4122	1.3982	1.3187	1.2376	1.2296

Table 7: Position errors of the models trained using different combinations of the loss function.

We compare the predictions of DP, DAPs, DBHP-S, DBHP-S and DBHP trained with different combinations of loss terms. Table 7 shows that DBHP achieves the best performance when all introduced loss functions are used. To be specific, the model trained with only L^d minimizes the MAE (Mean Absolute Error) between the positions predicted by DP and the ground truth, so DAPs based on the predicted derivatives are not trained. On the other hand, while models trained only with L^f or L^b predict DAPs better than the model trained only with L^d , the final performance of DBHP is inaccurate as the positions predicted by DP are not trained. Models trained with $L^d + L^f$ or $L^d + L^b$ achieve accurate predictions for both DP and DAPs, even though the weights between the three components are not trained. Lastly, the comparison between the model trained only with L^h and the proposed model indicates that directly enforcing the predictions of DP and DAPs with auxiliary loss terms such as L^d , L^f ,

and L^b actually helps DBHP achieve better performance. We speculate that the hybrid prediction works much better as the performance of each component improves.

A.4 Adaptation to Trajectory Forecasting

Forecasting future trajectories of multiple agents is another important task for various applications such as crowd navigation, autonomous driving, and behavior analysis (Kipf et al. 2018; Yeh et al. 2019; Li et al. 2020; Sun et al. 2022a). Especially, in team sports we are dealing with, predicting players’ future trajectories can serve as a tool for counterfactual analysis to evaluate players’ actual movements compared to the “average” movements for a given situation (Le et al. 2017; Teranishi et al. 2022; Wu and Swartz 2023).

Thus, we investigate our framework’s ability to adapt to the trajectory forecasting task. Since we cannot access the future information in the forecasting task, we deploy unidirectional LSTMs in DP and DBHP instead of the bidirectional ones. Also, we make DBHP obtain final predictions only based on DP and DAP-F, i.e.,

$$\hat{\mathbf{p}}_t^k = \lambda_t^{k,d} \hat{\mathbf{p}}_t^{k,d} + \lambda_t^{k,f} \hat{\mathbf{p}}_t^{k,f}. \quad (20)$$

Task	Imputation			Forecasting		
	50	100	200	50	100	200
F. Fill	4.1400	7.3255	9.6273	3.0578	6.1874	9.5810
BRITS	3.5872	5.5834	7.3686	6.9112	8.4179	10.6051
DP	0.2749	0.9417	2.1607	0.7035	2.9183	6.9366
DAP	0.2032	0.9011	2.1276	0.4987	2.5613	6.1439
DBHP	0.1460	0.8170	2.0256	0.4987	2.5608	6.1309

Table 8: Position errors of the predictions made by the models on the trajectory imputation and forecasting tasks. All settings share the same missing rate of 0.5. Note that the missing segment is in the middle of the given period for the imputation task, while it is fixed to the latter half of the period for the forecasting task.

To evaluate this DBHP forecaster, we compared its performance with that of some baselines (forward fills and BRITS) which are applicable to the forecasting task. Specifically, for the soccer dataset with window sizes 50, 100, and 200, we made the models observe the first half of the trajectories and predict the remaining half, respectively. For reference, we also measured the performance of the trajectory imputation models trained for the uniform missing scenario with a missing rate of 0.5.

According to Table 8, our framework consistently outperforms other forecasting baselines, but the performance is worse than the imputation task with the same setting. In particular, the DBHP forecaster does not improve that much from DAP-F’s performance as its imputation counterpart does. This is because it cannot leverage information from the future with the assistance of DAP-B. On the other hand, it seems that DAP-F forecasts trajectories more accurately than DP, demonstrating the effectiveness of using derivative information for trajectory forecasting.

One thing that we want to point out is that predicting players’ future trajectories is a stochastic task since there is great uncertainty in the dynamic nature of sports games. This implies that the predicted trajectories can be realistic even if they are very different from true trajectories in terms of position error. On this account, most studies (Yeh et al. 2019; Zhan et al. 2019; Li et al. 2020) for trajectory forecasting employ architectures based on Variational Autoencoder (VAE) (Kingma and Welling 2014) and make the model generate multiple outputs for the same input to encourage diversity. These are the key differences from our trajectory imputation task, which is rather deterministic in that the missing movement is somewhat determined given its start/end points and other players’ movements. We leave further fine-tuning our derivative-based framework and comparing its performance with state-of-the-art trajectory forecasters (Yeh et al. 2019; Zhan et al. 2019; Li et al. 2020; Sun et al. 2022a) as future work.